Simplified Design and Life Prediction of Rocket Thrust Chambers

J.S. Porowski,* W.J. O'Donnell,† M.L. Badlani,‡ B. Kasraie§
O'Donnell & Associates, Inc. Pittsburgh, Pennsylvania

and

H.J. Kasper¶
NASA Lewis Research Center, Cleveland, Ohio

An analytical procedure for predicting thrust chamber life is developed. The hot-gas wall ligaments separating the coolant and combustion gas are subjected to pressure loading and severe thermal cycling. The resulting stresses interact during plastic straining causing incremental bulging of the ligaments during each firing cycle. This mechanism of plastic ratcheting is analyzed and a method using a yield surface for combined bending and membrane loading is developed for determining the incremental permanent deflection and progressive thinning near the center of the ligaments. Fatigue and tensile instability are analyzed as possible failure modes. Results of the simplified analyses compare favorably with available experimental data and finite element analysis results for OFHC (Oxygen Free High Conductivity) copper. They are also in reasonably good agreement with experimental data for NARloy Z, a copper-zirconium silver alloy.

Nomenclature

a = axial length
A = material constant, also equation arbitrary positive scalar
D = rate of dissipation
E = modulus of elasticity
F = yield surface
$2H$ = thickness of ligament
k = $\sqrt{1-s^2}$
K = curvature
ℓ = width of ligament in hoop direction
m = generalized bending stress variable
M = bending moment in ligament
M_0 = yield bending moment
n = generalized hoop stress variable; also strain hardening exponent in stress strain law
N = hoop force in ligament; also number of cycles
N_0 = yield hoop force
P = pressure
s = generalized shear stress variable
S = shear force in ligament
S_0 = yield shear force
S_y = average yield stress in tension
$S_{y\min}$ = ligament yield strength for minimum $\alpha(T_i - T_0)$
$S_{y\max}$ = ligament yield strength for maximum $\alpha(T_i - T_0)$
t = ligament thickness
t_N = thinning after N cycles
$t_{\max}$ = maximum ligament thickness
$t_{\min}$ = minimum ligament thickness
T_i = average temperature of ligament
T_0 = average temperature of closeout wall
w = width of rib
α = coefficient of thermal expansion; also stress ratio σ_2/σ_1
γ = shear strain
δ = deflection per cycle
Δp = pressure difference between coolant pressure and combustion gas pressure
$\Delta\epsilon_{p_1}$ = plastic strain range in hoop direction
$\Delta\epsilon'_{p_1}$ = plastic strain range in hoop direction due to differential thermal expansion
$\Delta\epsilon''_{p_1}$ = correction to plastic strain range in hoop direction due to thermally induced bending
ϵ, ϵ_1 = hoop strain
ϵ_2 = axial strain
ϵ_3 = radial strain
$\epsilon_{1_{\text{avg}}}$ = average hoop strain in ligament
$\epsilon_{1_{\min}}$ = hoop strain in minimum ligament section
$\epsilon_{2_{\min}}$ = axial strain in minimum ligament section
$\bar{\epsilon}$ = effective strain
$\bar{\epsilon}_{\text{cr}}$ = critical effective strain
$\bar{\epsilon}_{\min}$ = effective strain in minimum ligament section
θ = generalized bending strain variable
λ = generalized hoop strain variable
ν = Poisson's ratio
σ_1 = hoop stress
σ_2 = axial stress
σ_b = bending stress
$\bar{\sigma}$ = effective stress
ϕ = generalized shear strain variable
$(\dot{})$ = rate

Received June 8, 1982; presented as Paper 82-1251 at the AIAA/SAE/ASME 18th Joint Propulsion Conference, Cleveland, Ohio, June 21-23, 1982; revision received Jan. 8, 1984.

*Executive Vice-President.
†President.
‡Manager, Applied Mechanics.
§Senior Engineer.
¶Aerospace Engineer.

Introduction

LIFE predictions of regeneratively liquid cooled rocket thrust chambers have been based on low cycle fatigue principles. Tests of thrust chambers, however,[1,2] revealed that coolant channel walls in the failed areas have exhibited progressive incremental thinning and bulging during the heating and cooling cycle associated with each firing. Ductile rupture often occurs before development of fatigue failure. Thus, material tensile instability was considered in addition to fatigue in the present structural evaluation.

The mechanism of inner layer incremental distortion can be investigated by inelastic finite element analysis. For cyclic histories, however, such analyses are difficult to perform and require extensive computer time. Their use for a single characteristic case is feasible and provides valuable information. Such methods, however, are not suitable for evaluating the effects of changing various design and operating parameters such as geometric configurations, material properties, pressures, and temperatures. More general methods which do not require lengthy inelastic finite element solutions are therefore needed.

The present work is thus aimed at analyzing the failure mode of the cyclically loaded thrust chamber, developing a simplified but conservative method for evaluating the strains and deformations, and providing a simplified design procedure for predicting its cyclic life.

Plug Nozzle Thrust Chamber

The plug nozzle thrust chamber of Fig. 1 is considered. The plug nozzle assembly consisting of the contoured centerbody and flanged cylinder is shown, along with cross-sectional details of the cylinder. The dimensions shown are for the experimental thrust chamber tested at NASA Lewis Research Center. Although the diameter and length of the nozzle are reduced, the dimensions of the cooling channels are similar to those for a full scale thrust nozzle. The inner wall of the cylinder contains axial flow coolant channels of constant cross section and is constructed from either OFHC copper, or half-hard Amzirc or NARloy-Z. The closeout wall is electroformed copper in all cases.

Typical firing cycle history data for the thrust chamber is illustrated in Fig. 2. The first cycle begins with a cooling period when the liquid hydrogen enters the channels. The uniform temperature of 53°R is reached before a sudden rise of temperature beginning at the ignition point of 1.5 s. The data refer to the critical section where failures were observed during testing. Only this section was considered in the analysis.

Development of a Simplified Analytical Procedure for Determining Hot-Gas Wall Deformation and Strain

The hot-gas wall ligaments separating the coolant and the combustion gas are subjected to pressure and severe thermal cycling. The resulting stresses interact during plastic straining causing incremental bulging directed radially inward. The

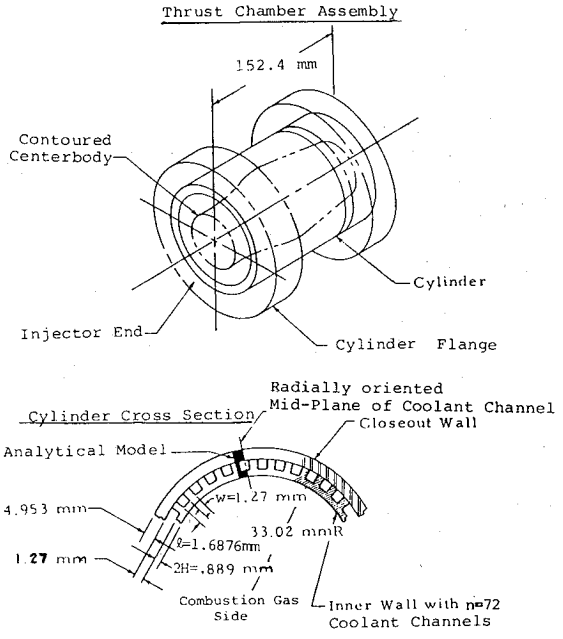

Fig. 1 Plug nozzle thrust chamber.

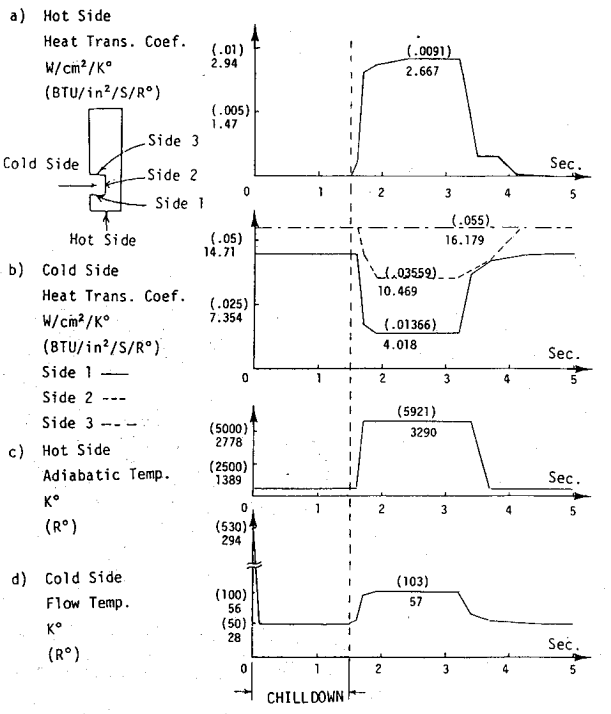

Fig. 2 Time histories of heat transfer coefficients and temperatures for a chilldown and firing cycle.

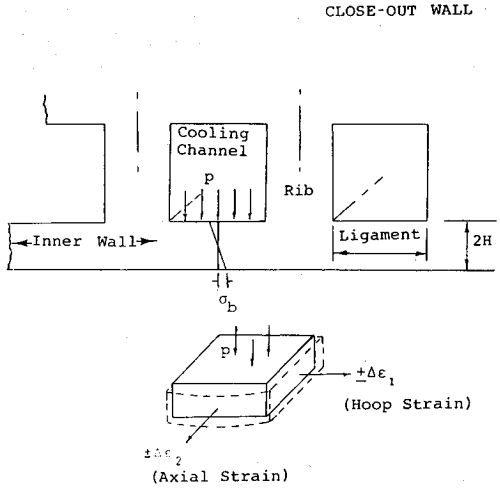

Fig. 3 Plastic ratcheting due to interaction of pressure-induced bending and cyclic in-plane straining.

mechanism of pressure induced ratcheting is illustrated in Fig. 3. Primary bending stresses persist during alternate in-plane cyclic straining resulting in a small repetitive incremental permanent deflection of the ligaments during each firing cycle.

The approach used to determine increments of plastic strain within the load cycles is explained in Fig. 4. The hoop force and bending moment acting on the rectangular cross section as shown in the top part of Fig. 4 are considered. The bar simulates the response of the ligament of a cooling channel between the two ribs. The bar is cyclically stretched and squeezed plastically in the presence of maintained bending. Note that the axial direction in the beam model corresponds to the hoop direction in the ligament.

To obtain a conservative bound on the plastic strain increments, strain hardening of the material is ignored.

The yield surface for a beam subjected to bending and hoop force is composed of two parabolas and is defined by the

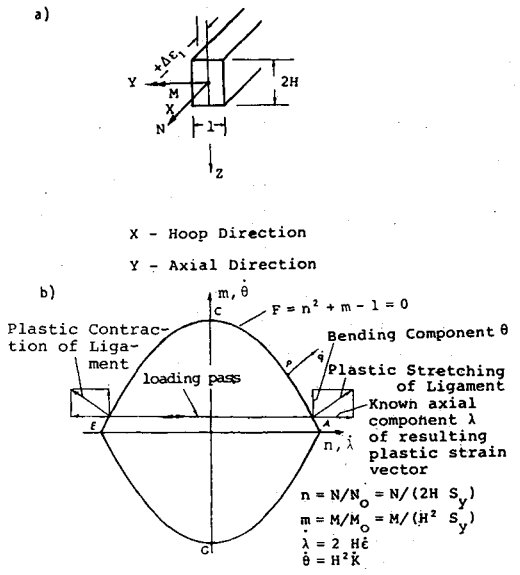

Fig. 4 Plastic ratchet increments in a bar of rectangular cross section subjected to sustained bending moment and cyclic axial strain.

relation:[3]

$$F = m + n^2 - 1 - 0 \tag{1}$$

where m and n are dimensionless variables defined by:

$$m = \frac{M}{M_0} \tag{2a}$$

$$n = \frac{N}{N_0} \tag{2b}$$

In the above, N and M denote the hoop force and bending moment, while N_0 and M_0 denote the yield hoop force and yield bending moment given by:

$$N_0 = 2HS_y \tag{3a}$$

$$M_0 = H^2 S_y \tag{3b}$$

for a rectangular beam of unit width, height $2H$ and yield stress S_y.

Plastic flow vectors $\dot{q}$ are normal to the yield curve. The curve is plotted using generalized stresses n and m related to the hoop and bending tractions, respectively. The associated generalized strain rates $\dot{\lambda}$ and $\dot{\theta}$ are defined by the average hoop strain rate $\dot{\epsilon}$, and the rate of curvature of the bent bar, $\dot{K}$, respectively. If hoop increment of plastic strain is known, the corresponding increment of curvature is defined by the slope of the yield surface and can be determined (based on normality of resulting strain rate vector $\dot{q}$) as shown in the bottom part of Fig. 4.

The generalized strain rates can be obtained by partial differentiation of Eq. (1) as follows:

$$\dot{\lambda} = A\frac{\partial F}{\partial n} = 2nA \tag{4a}$$

$$\dot{\theta} = A\frac{\partial F}{\partial m} = A \tag{4b}$$

where A is an arbitrary positive scalar. Thus, for the interaction of hoop and bending loads, the relation between $\dot{\lambda}$ and $\dot{\theta}$ components of the $\dot{q}$ vector is simply:

$$\frac{\dot{\theta}}{\dot{\lambda}} = \frac{1}{2n} \tag{5}$$

For known values of bending m which remain constant within the cycle, n can be obtained from the yield line Eq. (1). Hoop increments of plastic strain are being reversed within two halves of the thermal cycle. However, plastic increments of curvature resulting within each half of the thermal cycle are of the same sign. Thus they accumulate, causing ratchet bulging of the cooling channel wall.

With high pressures in the cooling channels, the model of the nozzle must also include shear stress τ. The method of analysis is analogous. However, the solution includes also generalized shear stress and the corresponding shear strain.

The yield surface based on Tresca's yield criterion is then given by Peterson, et al.[4]

$$F = m + \frac{n^2}{k} - k = 0 \tag{6a}$$

where

$$k = \sqrt{1 - s^2} \tag{6b}$$

and $s = 2\tau/S_y$ is the dimensionless shear stress.

Using the normality law:

$$\dot{\lambda} = A\frac{\partial F}{\partial n} = 2An \tag{7a}$$

$$\dot{\theta} = A\frac{\partial F}{\partial m} = A\sqrt{1 - s^2} \tag{7b}$$

$$\dot{\phi} = A\frac{F}{s} = A\left(2s - \frac{ms}{\sqrt{1 - s^2}}\right) \tag{7c}$$

the proportions between the strain components are thus:

$$\frac{\partial F}{\partial m} : \frac{\partial F}{\partial n} : \frac{\partial F}{\partial s} = \sqrt{1 - s^2} : (2n) : \left(2s - \frac{ms}{\sqrt{1 - s^2}}\right) \tag{8}$$

The generalized variables λ and θ can be related to the hoop strain, curvature, and shear strain by considering the rate of dissipation D given by:[3]

$$D = M\dot{K} + N\dot{\epsilon} + \dot{\gamma}S \tag{9}$$

where M, N, and S denote the bending moment, hoop force, and shear force, respectively, and $\dot{K}$, $\dot{\epsilon}$ and $\dot{\gamma}$ denote the curvature rate, hoop strain rate, and shear strain rate, respectively.

Using Eq. (2), Eq. (9) can be written as

$$D = mM_0\dot{K} + nN_0\dot{\epsilon} + sS_0\dot{\gamma} \tag{10a}$$

where

$$s = \frac{S}{S_0} = \frac{2\tau}{S_y} = \frac{S}{HS_y} \tag{10b}$$

since the cross-sectional area for unit width equals $2H$.

Then, using Eqs. (3) and (10b):

$$D = S_y\left[m(H^2\dot{K}) + n(2H\dot{\epsilon}) + s(H\dot{\gamma})\right] \tag{11a}$$

$$= S_y\left[m\dot{\theta} + n\dot{\lambda} + s\dot{\phi}\right] \tag{11b}$$

Thus the relationship between the generalized strain rates and the hoop strain rate, curvature rate and shear strain rate are,

respectively

$$\dot{\lambda} = 2H\dot{\epsilon} \tag{12a}$$

$$\dot{\theta} = H^2\dot{K} \tag{12b}$$

$$\dot{\phi} = H\dot{\gamma} \tag{12c}$$

For known increments of hoop strains and given values of m and s, the remaining components of strain are determined by relation (8). Since the load point must remain on the yield surface, the given values of m and s determine n, which is obtained from Eq. (6a).

It can be shown from the generalized yield surfaces derived[4] that though the yield surface given by Eq. (6a) is derived for a uniaxial model, it also holds for biaxial conditions when $n_2 < n_1$ [$n_1 = n$ = hoop stress variable in Eq. (6a)] and m and s are small, as in the present case. Thus the generalized strain relationships derived above are also applicable for the biaxial case.

For the complete cycle, the plastic strain generated by the temperature difference during heat-up in the hoop direction is fully reversed when the temperature becomes uniform at the end of the cycle. Thus,

$$\epsilon = \epsilon_1 = 2\Delta\epsilon_{p_1} \tag{13}$$

where $\Delta\epsilon_{p_1}$ is given by the sum of the plastic strain range due to differential thermal expansion $\Delta\epsilon'_{p_1}$, and the correction due to thermally induced bending, $\Delta\epsilon''_{p_1}$.

Since the thickness of the ligament is small with respect to the thickness of the closeout wall, the elastic deformation of the closeout wall can be disregarded. Denoting the average temperatures of the ligament and closeout wall by T_i and T_0, respectively, the hoop strain range due to differential thermal expansion is given by:

$$\Delta\epsilon'_{p_1} = \left[(T_i\alpha_i - T_0\alpha_0)_{\max} - (T_i\alpha_i - T_0\alpha_0)_{\min}\right] - \left(S_{y\max} + S_{y\min}/E\right) \tag{14}$$

where α_i and α_0 are the thermal expansion coefficients of the ligament and closeout, respectively, and $(T_i\alpha_i - T_0\alpha_0)_{\max}$ and $(T_i\alpha_i - T_0\alpha_0)_{\min}$ are the maximum and minimum thermal strains, respectively, that occur during the loading cycle. $S_{y\max}$ and $S_{y\min}$ are, respectively, the ligament material absolute yield strengths corresponding to the ligament average temperatures at the times in the cycle when $(T_i\alpha_i - T_0\alpha_0)_{\max}$ and $(T_i\alpha_i - T_0\alpha_0)_{\min}$ are calculated.

The ligaments are subjected to severe thermal straining due to the temperature difference between the ligament and closeout wall. Thus $\Delta\epsilon'_{p_1}$ accounts for the major portion of the plastic strain range in the hoop direction. However, there is also an essential temperature drop through the wall of the ligament. Since the ligament is constrained at the ends, this causes bending.

The thermally induced bending, though acting only for a short portion of the cycle, may enhance the ratchet strain. Its effect may be assessed by computing the elastic energy of the thermally induced bending stresses and correcting the hoop strain accordingly. Conservatively assuming that all of the available elastic energy goes into plastic straining of the ligament:[5]

$$\Delta\epsilon''_{p_1} = \frac{E(\alpha\Delta T)^2}{12(1-\nu)^2 S_y} \tag{15}$$

where (ΔT) is the temperature drop across the ligament.

From Eqs. (7), (12), and (13) it can be shown that the curvature and shear strain are, respectively

$$K = \frac{2\sqrt{1-s^2}}{n}\,\frac{(\Delta\epsilon_{p_1})}{H} \tag{16}$$

and

$$\gamma = 2\left(2s - \frac{ms}{\sqrt{1-s^2}}\right)\frac{(\Delta\epsilon_{p_1})}{n} \tag{17}$$

In both these equations

$$\Delta\epsilon_{p_1} = \Delta\epsilon'_{p_1} + \Delta\epsilon''_{p_1} \tag{18}$$

where $\Delta\epsilon'_{p_1}$ and $\Delta\epsilon''_{p_1}$ are given by Eqs. (14) and (15), respectively.

The curvature and shear strain as determined from Eqs. (16) and (17) for each cross section can then be integrated along the length of the ligament to obtain the bending and shear deflections. Once the total deflection is known, the corresponding thinning of the ligament is calculated by assuming that the volume of the material remains constant.

Experimental evidence shows that the deformed shape of the ligament can be approximated by a linear variation in thickness as shown in Fig. 5. If δ denotes the deflection per

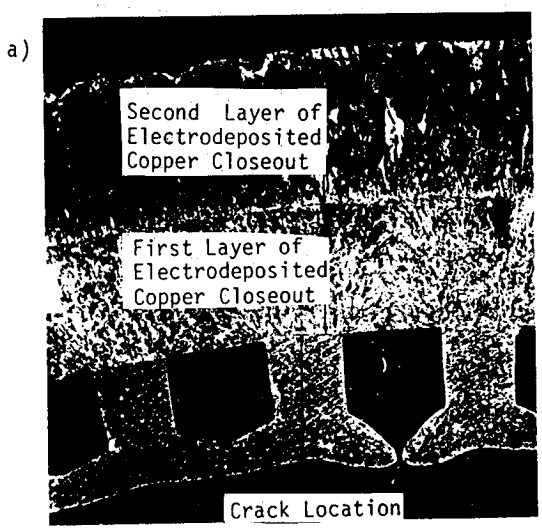

Fig. 5a Typical cooling channel wall failure.

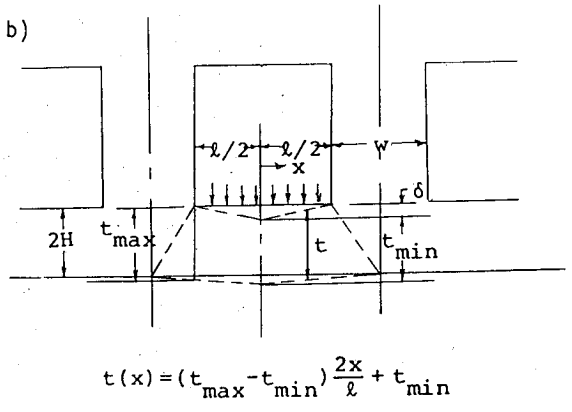

Fig. 5b Ligament linear thinning model.

cycle, the thinning after N cycles is then given by:

$$t_N = \frac{N\delta w}{(\ell + w)} \tag{19}$$

Note that even though the incremental deflection remains constant, the incremental strain at the center of the ligament increases with each cycle, due to ligament thinning.

Development of Failure Mode Evaluation Criterion

The ligaments are subjected to incremental plastic deformations during each firing cycle of the thrust chamber. The geometry of these ligaments changes as the incremental strains accumulate. They are subjected to incremental inward bending and simultaneously to a progressive thinning near the center of the ligament. Both fatigue damage and the tensile stability of the material are affected by local geometry changes. The strain range at the minimum cross section of the ligament intensifies with progressing distortion and thinning. Plastic tensile instability occurs when the incremental strain hardening of the deforming metal is less than the incremental increase of true stress, due to local thinning. Once conditions of tensile instability are reached, further stretching occurs as minimum ligament section necking. The pressure in the chamber causes ultimate failure of the necked ligament.

Plastic Instability—Necking

The plastic tensile instability of the ligament in the displacement controlled thermal cyclic strain field is analyzed first by considering the ligament as a biaxially loaded shell subjected to monotonic tensile straining in the hoop and axial directions.

For a biaxially stretched sheet, the Mises yield condition is:

$$\bar{\sigma} = \sigma_1 (1 - \alpha + \alpha^2)^{\frac{1}{2}} \tag{20}$$

where $\bar{\sigma}$ is the effective stress, α is the stress ratio σ_2/σ_1, and σ_1 and σ_2 are principal stresses in the hoop and axial directions, respectively.

In the present analysis, elastic strains will be neglected and the Levy-Mises rule gives:

$$\frac{d\epsilon_1}{2-\alpha} = \frac{d\epsilon_2}{2\alpha - 1} = \frac{-d\epsilon_3}{1+\alpha} = \frac{d\bar{\epsilon}}{2(1-\alpha+\alpha^2)^{\frac{1}{2}}} \tag{21}$$

where

$$d\bar{\epsilon} = \sqrt{\tfrac{2}{3}\left(d\epsilon_1^2 + d\epsilon_2^2 + d\epsilon_3^2\right)^{\frac{1}{2}}} \tag{22}$$

In the above, $d\bar{\epsilon}$ is the increment of effective strain and $d\epsilon_1$, $d\epsilon_2$, and $d\epsilon_3$ are the strain increments in the hoop, axial, and radial (thickness) directions, respectively.

For proportional loading, the stress ratio remains constant and Eq. (21) can be integrated to give the total strains:

$$\frac{\epsilon_1}{2-\alpha} = \frac{\epsilon_2}{2\alpha - 1} = \frac{-\epsilon_3}{1+\alpha} = \frac{\bar{\epsilon}}{2(1-\alpha+\alpha^2)^{\frac{1}{2}}} \tag{23}$$

Defining instability to occur when the hoop force F passes through a maximum, i.e.,

$$dF = d(2Ha\sigma_1) = 0 \tag{24}$$

where $2H$ denotes the thickness of the ligament and a its axial length. Equation (24) is differentiated to give

$$\frac{d\sigma_1}{\sigma_1} = -\frac{da}{a} - \frac{dH}{H} = -d\epsilon_2 - d\epsilon_3 = d\epsilon_1$$

(from incompressibility) (25)

Using Eq. (21) and noting that for proportional stressing $d\sigma_1/\sigma_1 = d\bar{\sigma}/\bar{\sigma}$, the condition for instability is given by

$$\frac{d\bar{\sigma}}{d\bar{\epsilon}} = \frac{(2-\alpha)\bar{\sigma}}{2(1-\alpha+\alpha^2)^{\frac{1}{2}}} \tag{26}$$

If the stress-strain law is

$$\bar{\sigma} = A\bar{\epsilon}^n \tag{27}$$

where A and n are material constants, then on differentiating

$$\frac{d\bar{\sigma}}{d\bar{\epsilon}} = \frac{n\bar{\sigma}}{\bar{\epsilon}} \tag{28}$$

Thus the critical effective strain is:

$$\bar{\epsilon}_{cr} = \frac{2n(1-\alpha+\alpha^2)^{\frac{1}{2}}}{(2-\alpha)} \tag{29}$$

and the critical strain in the minimum ligament section from Eq. (23) is then:

$$\epsilon_{1_{cr}} = n \tag{30}$$

For cyclic loading, the compressive straining of a ligament at the beginning of the loading cycle is followed by tensile strains. In each loading cycle the ligament accumulates plastic strain. The net increments in the hoop and radial directions occur at the end of the cycle when the axial strain is zero. Thus, the limits of material stability can be approximated by the analysis for plane strain conditions. The plastic strains in the hoop direction $d\epsilon_1$, and in the radial direction $d\epsilon_3$ satisfy the condition of incompressibility. Since $d\epsilon_2 = 0$:

$$d\epsilon_1 = -d\epsilon_3 \tag{31}$$

Now,

$$\epsilon_3 = \ell n\left(\frac{t}{2H}\right) \tag{32}$$

where $2H$ denotes the original ligament thickness and t the ligament variable thickness. Then using Eqs. (30), (31), and (32), the critical thickness at instability is given by:

$$t_{cr} = 2He^{-n} \tag{33}$$

Strain Range—Fatigue

For fatigue calculations, the maximum local hoop strain range at the minimum ligament section can be obtained from the average hoop strain range by integration if the geometry of the distorted ligament is known. As mentioned earlier, tests indicate that the deformed shape of the ligament can be approximated by a linear function as shown in Fig. 5. Thus, the thickness variation can be written as:

$$t(x) = (t_{max} - t_{min})\frac{2x}{\ell} + t_{min} \tag{34}$$

where t_{max} and t_{min} are as shown in the figure. Now the average strain in the hoop direction is given by

$$\epsilon_{1_{avg}} = \frac{2}{\ell}\int_0^{\ell/2} \epsilon_1(x)\,dx \tag{35}$$

From equilibrium of forces in the hoop direction

$$\sigma_1(x)t(x) = \sigma_{1_{min}} t_{min} \tag{36a}$$

Using Eqs. (20), (27), and (23), Eq. (36a) is written as

$$\epsilon_{l}(x)^{n} t(x) = \epsilon_{l_{\min}}^{n} t_{\min} \tag{36b}$$

Substituting for $\epsilon_l(x)$ into Eq. (35), the relation between the average strain and local strain is given by:

$$\epsilon_{l_{\text{avg}}} = \frac{2\epsilon_{l_{\min}}}{\ell} \int^{\ell/2} \left\{ \frac{t_{\min}}{t(x)} \right\}^{1/n} dx \tag{37}$$

Substituting for $t(x)$ from Eq. (34), integrating and solving for $\epsilon_{l_{\min}}$ gives:

$$\epsilon_{l_{\min}} = \epsilon_{l_{\text{avg}}} \frac{n-1}{n} \left(\frac{t_{\max}}{t_{\min}} - 1 \right) \left[\left(\frac{t_{\max}}{t_{\min}} \right)^{\frac{n-1}{n}} - 1 \right]^{-1} \tag{38}$$

$\epsilon_{l_{\min}}$, the local strain in the minimum ligament section, intensifies with each cycle.

Using the conditions of incompressibility, the effective strain range in the minimum ligament section for entering the fatigue curve is then:

$$\bar{\epsilon}_{\min} = \frac{2}{\sqrt{3}} \sqrt{\epsilon_{l_{\min}}^2 + \epsilon_{l_{\min}} \epsilon_{2_{\min}} + \epsilon_{2_{\min}}^2} \tag{39}$$

where $\epsilon_{l_{\min}}$ is given by Eq. (38) and $\epsilon_{2_{\min}}$, the axial strain in the minimum ligament section, is

$$\epsilon_{2_{\min}} = \alpha(T_i - T_0) \tag{40}$$

For the linear variation assumed, the thicknesses $t_{\min}$ and $t_{\max}$ after the N^{th} cycle are given by:

$$t_{\min} = \frac{2H(l+w) - N\delta w}{(l+w)} \tag{41}$$

$$t_{\max} = \frac{2H(l+w)^2 + N\delta lw}{(l+w)^2} \tag{42}$$

where δ is the deformation per cycle.

Equations (38) through (42), along with the fatigue curve, are then used to determine the fatigue life. However, since $\epsilon_{l_{\min}}$ changes with each cycle, a numerical procedure is necessary for performing the calculations to determine fatigue life. A FORTRAN program, therefore, was written and used for determining the cycles to failure.

Thrust Chamber Life Predictions

The results obtained using these analyses can be used to predict the life of the thrust chamber. For small ligament distortion, it can be conservatively assumed that the incremental thinning of the ligament remains constant during subsequent cycles. The numbers of cycles to failure can then be bounded from below by considering the number of cycles needed to reduce the thickness of the ligament below the critical value resulting in tensile instability, or by considering the fatigue damage of the gradually thinned ligament, whichever is more limiting. For OFHC copper, this bounding technique provides a realistic evaluation of the cycles to failure observed in experiments where failure was due to tensile instability.

For NARloy Z, the thinning gradually diminishes in consecutive cycles due to material hardening, and the fatigue mode of failure is limiting. It has been demonstrated theoretically[6,7] that for kinematically hardening materials, the cyclically loaded structure always achieves the condition of alternating plastic straining if there is no limit on the hardening capacity and the changes of geometry can be ignored. The net increment of plastic ratchet strain vanishes after sufficient hardening. The amount of plastic strain accumulation needed to achieve such plastic shakedown can be theoretically determined. For real materials with limited hardening capacity and less than ideal kinematic behavior, the stable cyclic state occurs at much larger accumulated strains than for an ideal kinematically hardening material and may never be achieved. Materials more closely obeying the theoretical concept of kinematic hardening can be expected to fail due to fatigue since retarded thinning allows the material to be exposed to more fatigue cycles, as in the case of NARloy Z.

The number of cycles at which thinning stops is related to the strain hardening parameter n. Hypothesizing a power relationship, the following empirical criterion was obtained using the results of Armstrong:[8]

$$N_T = 750n^{1.25} \tag{43}$$

where N_T denotes the number of cycles at which thinning stops.

If the number of cycles to reach the critical thickness for plastic tensile instability is less than N_T for a particular material, tensile stability is the limiting failure mode. Once thinning stops, the effective strain range remains constant, and the further fatigue damage can easily be evaluated.

Finite Element Analysis

The MARC[9] general purpose finite element computer program was used for the thermal and mechanical part of the analysis. The MARC program was adapted to analyze the fast thermal and pressure thrust nozzle transient. Optimized selection of the time and load steps was used for the thermal and elastic-plastic analyses.

The finite element inelastic analysis confirmed the fact that the simplified model developed herein includes the essence of the physical behavior of the ligament. Moreover, the results of the finite element analysis were employed in calibrating the thermal model of the ligament.

The finite element mesh used for the analysis is shown in Fig. 6. A description of the model and details of the finite element analysis for the case of OFHC copper are given by Porowski, et al.[5]

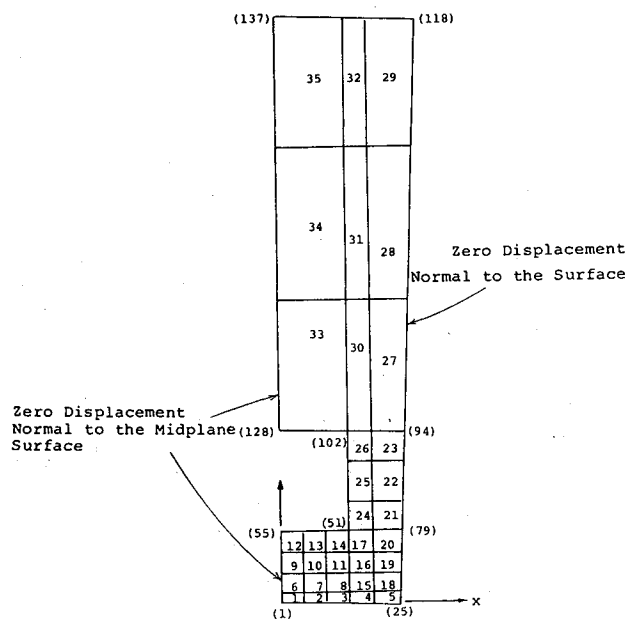

Fig. 6 Finite element model.

Table 1 Comparison of analytical vs finite element results (residual deflection after one cycle)

Deflection of pressure surface/cycle	
Analytical results	Finite element results
0.00029 in. (0.00737 mm)	0.00027 in. (0.00686 mm)

Comparison of Results

The numerical results obtained for OFHC copper, using the simplified analysis procedure developed herein, are compared with the finite element results in Table 1. The results are seen to be in good agreement. The life prediction of 103 cycles for OFHC copper and 833 cycles for NARloy Z was also in general agreement with typical experimental results[2] that ranged from 58 to 220 cycles for OFHC copper and 556 to 688 cycles for NARloy Z, indicating that the simplified design procedure can be used for predicting the life of the thrust chamber without performing detailed inelastic analysis.

Conclusions

A simplified design procedure for predicting thrust chamber life is developed herein. The method uses a yield surface for combined bending and membrane loading to determine the incremental inward bulging and progressive thinning near the center of the ligaments at the inner liner of the thrust chamber. Failure analyses indicate that plastic tensile instability is the dominant mode of failure for OHFC copper. Both fatigue and plastic tensile instability must be analyzed for NARloy Z to determine the limiting failure mode. Results of the simplified analyses are shown to compare favorably with experimental data and finite element analysis results for OFHC copper. Results are also in reasonably good agreement with experimental data for NARloy Z.

References

[1] Hannum, N.P., Kasper, H.J., and Pavli, A.J., "Experimental and Theoretical Investigation of Fatigue Life in Reusable Rocket Thrust Chambers," NASA TM X-73413, Lewis Research Center, Cleveland, Ohio, July 1976.

[2] Quentmeyer, R.J., "Experimental Fatigue Life Investigation of Cylindrical Thrust Chambers," NASA TM X-73665, Lewis Research Center, Cleveland, Ohio, July 1977.

[3] Hodge, P.G., Jr., *Plastic Analysis of Structures*, McGraw Hill Book Company, New York, 1959.

[4] Peterson, D.B., Kroenke, W.C., Stokey, W.F., and O'Donnell, W.J., "Generalized Yield Surfaces for Plates and Shells," WRC Bulletin No. 250, July 1979.

[5] Porowski, J.S., Badlani, M.L., Kasraie, B., O'Donnell, W.J., and Peterson, D., "Development of a Simplified Procedure for Thrust Chamber Life Prediction," NASA CR-165585, Contract NAS3-22649, NASA Lewis Research Center, Cleveland, Ohio, Oct. 1981.

[6] Frederick, C.O. and Armstrong, P.J., "Convergent Internal Stresses and Steady Cyclic States of Stress," *Journal of Strain Analysis*, Vol. 1(2), 1966, p. 154.

[7] Halphen, M.B., "L'accomodation des structures elastoplastiques a ecrouissage cinematique," C. R. Académie des Sciences, T 283, Paris, October 1976, p. 799.

[8] Armstrong, W.H., "Structural Analysis of Cylindrical Thrust Chamber," Final Report, Volume II, NASA CR-165241, Contract NAS3-21953, Lewis Research Center, Cleveland, Ohio, March 1981.

[9] *MARC General Purpose Finite Element*, MARC Analysis Research Corporation, Palo Alto, Calif., Rev. 1980.